A POTENTIAL FRAMEWORK FOR EXPLOITING THE BENEFITS OF HIGH-TOUGHNESS STEEL

RYAN SHERMAN

WILLIAM COLLINS

ROBERT CONNOR

BIOGRAPHY

Dr. Ryan Sherman, P.E. is an Assistant Professor at the University of Nevada, Las Vegas. He received his BS from Michigan Technological University, followed by his MS and PhD from Purdue University. He has also worked as a Research Engineer at Purdue University completing field and laboratory research on steel bridge and ancillary highway structures. His research and teaching interests encompass large-scale structural testing and field monitoring of steel structures.

Dr. William Collins, P.E. is an Assistant Professor at the University of Kansas. He received his BS, MS, and PhD from Virginia Tech, focusing his studies on steel bridge behavior and performance. After completing his doctoral studies he worked as a Research Engineer at Purdue University. His research and teaching interests focus on steel structures, with an emphasis on fatigue and fracture behavior.

Dr. Robert Connor has over 25 years of experience in the fatigue and fracture evaluation of steel bridges. He is currently a Professor in the Lyles School of Civil Engineering and Director of the S-BRITE Center at Purdue University. During his career, he has researched fabrication flaws, fatigue cracking, brittle fractures, and developed repair strategies for structures for a variety of agencies including state DOT, rapid transit authorities, construction companies, and structural consultants.

SUMMARY

Steel bridge systems historically classified as non-redundant have been used in the United States since the late 1800's because of their inherent structural efficiency and economy. Unfortunately, the stringent in-service 24-month hands-on inspection mandate has effectively discouraged the use of systems traditionally considered to be non-redundant. In the 40 years following the introduction of the original steel bridge fracture requirements, significant advances have been made in design, materials, fabrication, and inspection. However, no provisions currently leverage the advantage of advanced materials, specifically modern, high-toughness steel.

Current understanding of fracture mechanics allows for the calculation of critical flaw sizes and fatigue crack-growth life, thereby allowing engineers to set rational in-service inspection intervals. Studies examining high-toughness materials have worked towards the development of an integrated approach to prevent steel bridge fracture. The following paper discusses the parameters and assumptions involved in establishing a rational inspection interval. Additionally, a parametric analysis is conducted to demonstrate the impact various assumptions and parameters have on the final interval. Ultimately, results demonstrate a potential framework for exploiting the benefits of high-toughness steel resulting in rational inspection intervals.

A POTENTIAL FRAMEWORK FOR EXPLOITING THE BENEFITS OF HIGH-TOUGHNESS STEEL

Introduction and Background

The original AASHTO Fracture Control Plan (FCP), released in 1978, was a comprehensive guide specification aimed at reducing the likelihood of brittle fracture (1). Specification requirements covered design review, material toughness, fabrication, welder certification, and weld inspector qualifications. Through subsequent revisions, the FCP was divided into separate specifications designed to address material toughness, design, fabrication, weld inspection, and in-service inspection independently. Design and material requirements are detailed in the *AASHTO LRFD Bridge Design Specification* and ASTM A709-17 (2,3). Fabrication and shop inspection requirements are contained in Clause 12 of the *AASHTO/AWS D1.5M/D1.5 Bridge Welding Code* (4). In-service inspection requirements are prescribed in the *AASHTO Manual for Bridge Evaluation* (5). As a result, currently no single, integrated plan addressing steel bridge fracture exists.

The excellent service record suggests current practice has been successful in preventing failure due to brittle fracture. However, the FCP was not developed to ensure any specific performance level, crack tolerance, or overall reliability. Advances in the understanding of fracture mechanics, material and structural behavior, fatigue crack initiation, fatigue crack growth, fabrication technology, and inspection technology have allowed other industries to address fracture in a more integrated manner. As such, it is now possible to create an integrated FCP, combining the original intent of the 1978 FCP, with modern advances. Further, an integrated FCP will provide an economic benefit to owners. In summary, an integrated FCP encompassing material, design, fabrication, and inspection can make fracture no more likely than any other limit state; ultimately, allowing for a better allocation of owner resources and increased steel bridge safety.

The following presents a framework for developing an integrated FCP with rational inspection intervals. Different assumptions are explored for parameters influencing the inspection type and frequency. Finally, a parametric analysis is conducted for high-toughness steel to demonstrate the impact varying different assumptions have on the fatigue crack life.

Previous Research

In 1994, collaborative efforts between the steel industry, FHWA, and the Navy worked to develop high performance steel (HPS) for bridge applications. Through alloying and heat treatment processes, HPS gained desirable material characteristics, including high-strength, improved weldability, corrosion resistance, and increased toughness (6).

The improved toughness of HPS was demonstrated by experimental testing of HPS 70W and HPS 100W (7). Full-scale I-girder fracture experiments were performed in addition to fracture mechanics-based material tests. The study concluded HPS 70W was capable of reaching the limit state of yield on the net section, while HPS 100W could not. Compared to conventional bridge steels, test results indicated HPS would result in increased critical crack sizes for plate girders due to the higher toughness.

Further HPS material characterization was performed aimed at quantifying the CVN impact energy, static and dynamic fracture toughness, and crack arrest toughness (8). The study included 636 fracture toughness tests from five HPS 70W plates and three HPS 100W plates. Additionally, the study evaluated the applicability of the master curve methodology to historic bridge steel data sets (8,9). Fracture toughness results indicated HPS 70W could tolerate crack sizes 20 times larger than a material just meeting the current AASHTO material toughness specification, while HPS 100W was able to tolerate crack sizes three times larger than the specification. Further, based on the master curve, adequate toughness was available to achieve a one percent probability of cleavage fracture prior to attaining net section yield for some crack geometries.

Large-scale testing was conducted to demonstrate and quantify the performance benefits of modern high-toughness steel (10). The project was comprised of material characterization testing, full-scale fracture testing of steel bridge axial and bending members,

three-dimensional finite element modeling, and an analytical parametric study. Three heats of high-toughness steel were tested including grades 50W and HPS 70W. All material had an average CVN impact energy of 125 ft-lbf at the test temperature. Results from the research formed the basis of the current paper and demonstrate a potential framework for exploiting the benefits of high-toughness steel resulting in rational inspection intervals, a better allocation of owner resources, and increased steel bridge safety.

Framework

Integrated Fracture Control Plan

The essence of an integrated FCP is to prevent fracture through a series of interrelated components, which influence each other in a rational and quantifiable way. Such a process starts with design and continues through the entire life of a structure. For new steel bridges, the required components of an integrated FCP include design considerations, material properties, fabrication guidelines, and in-service inspection.

An integrated FCP approach needs to be developed and adopted at the outset of design. Early considerations regarding design details and live load stress range can directly impact the overall success. For example, designing a structure with a low live load stress range and selecting highly fatigue resistant details could effectively eliminate the likelihood of fatigue crack growth during the life of the bridge. Design is the foundation of the integrated FCP because initial decisions directly influence long-term success.

The mechanical properties of the design material are an imperative part of the integrated FCP. Material properties influence the tolerable crack size of a member. Tolerable flaw size is directly related to in-service inspection capabilities; the larger the flaw, the more likely it is to be detected during an inspection. As such, when specifying material properties for a structure the designer is actually setting the critical flaw size required to be detected during an in-service inspection. Tying material properties to in-service inspection is fundamentally how the integrated FCP protects against fracture.

The current FCP is fabrication-based and can be incorporated into an integrated approach. Inspection requirements and acceptance criteria for welds produced during fabrication already exist. While the present criteria are solely based on workmanship, an integrated FCP would tie the acceptance and rejection criteria to initial flaw sizes, crack growth rates, and variability in detection of certain inspection techniques (4). Establishing acceptance criteria based on fracture mechanics allows the timing of in-service inspection cycles to be rationally established.

The inspection process can be defined by method, rigor, and interval. Method refers to the type of inspection being performed, such as visual, dye penetrant, magnetic particle, ultrasonic, or radiographic. Rigor refers to the rate at which the method is applied. For example, a welded joint might be inspected 100% visually and 20% using magnetic particle inspection. Interval refers to the length of time between inspections. Currently, the maximum in-service inspection interval is mandated as 24 months with 48 months in some special cases for routine safety inspections; however, fracture critical members require a hands-on inspection at an interval not to exceed 24 months (5,11). While the current approach is based solely on past experience and engineering judgement, an integrated FCP applies knowledge of design, loading, environment, probability of detection (POD), and other characteristics to quantitatively set the inspection type and frequency. With an integrated approach, the finite resources for inspection, maintenance, and repair are most efficiently appropriated.

Assumptions

A variety of parameters influences the calculation of a rational inspection interval. Each parameter has multiple variables uniquely influencing the final result. Engineers working to establish appropriate inspection criteria must make decisions and assumptions regarding the application of the parameters. The parameters are presented here grouped under three overarching categories: fracture toughness, fracture mechanics, and fatigue life. The following sections describe the parameters and associated variables. Descriptions include the values used in the following framework example.

Toughness Level

The value of fracture toughness used in an engineering assessment is extremely influential on the critical flaw size. Currently, there is no directly

specified level of fracture toughness required for steel bridges. To establish a suitable toughness level, assumptions are required for the toughness correlation, test temperature, material thickness, probability of failure (POF), and loading rate.

Correlation

Material toughness requirements for bridge steels are applied through a specified minimum Charpy V-notch (CVN) impact energy (2,3). However, CVN testing does not provide a quantifiable measure of fracture toughness directly applicable in an engineering assessment. Therefore, correlation methods have been proposed in the literature relating CVN impact values to fracture toughness, K, values. Previous research examined 29 variations of correlation methods for applicability to historic bridge steel (12). Two of the 29 methods are presented herein.

Barsom and Rolfe Two-Stage

Forming the basis of the AASHTO toughness specifications, the Barsom and Rolfe Two-Stage CVN-K method involves a toughness correlation followed by a temperature adjustment. In the first stage, the correlation relates CVN impact toughness to dynamic fracture toughness, K_{Id}. The correlation is often represented in the following simplified form:

$$K_{Id} = 12\sqrt{CVN}$$

where K_{Id} is dynamic fracture toughness in ksi√in and *CVN* represents CVN impact energy in ft-lbf. The influence of loading rate on fracture toughness can be represented by a temperature shift. In the second stage, the correlation adjusts the temperature of the fracture toughness value to convert the dynamic test rate to a static fracture toughness value. The temperature shift is represented by:

$$T_{shift} = 215 - 1.5\sigma_{ys}$$

where the T_{shift} is the temperature adjustment in degrees Fahrenheit, and σ_{ys} is the material yield strength in ksi. Although not used in the present example, the correlation is presented because of its ubiquity within the steel bridge community.

BS 7910

The British Standards Institute presents a number of correlation methods for evaluating fracture toughness in Annex J of *BS 7910: Guide to Methods for Assessing the Acceptability of Flaws in Metallic Structures* (13). The methods include correlations between CVN impact energy and material reference temperature, T_o, as well as between CVN and K values. The CVN-K correlation used in the present example is a direct conversion of the form:

$$K = \left[\left(12.7\sqrt{CVN} - 18.2\right)\left({}^{1}/_{B}\right)^{0.25}\right] + 18.2$$

where *K* is static fracture toughness in ksi√in, *CVN* is impact energy in ft-lbf, and *B* is material thickness in in. The selected correlation corresponds to a five percent probability of specimen failure, meaning only five percent of fracture toughness specimens sampled from the material in question would exhibit fracture toughness lower than the predicted value.

Test Temperature

Material toughness is highly dependent on temperature; therefore, determining an appropriate value for material qualification testing is critical to an integrated fracture control plan. Due to the temperature shift built into the Barsom and Rolfe Two-Stage correlation, the current AASHTO material toughness specifications require CVN testing at temperatures significantly warmer than the expected bridge service temperature. In comparison, other correlations, such as the above BS 7910 method, permit CVN testing at the temperature of the fracture toughness prediction. Testing at the specified minimum service temperature (MST) provides a transparent methodology for assessing material fracture toughness.

Thickness Correction

Due to the statistically higher incidence of fracture initiation sites in thick plate, fracture toughness of ferritic steels is known to be dependent on material thickness (14). Thus, a thick plate will exhibit lower fracture toughness than a thin plate of the same material. Current AASHTO material requirements do not acknowledge a thickness dependence and inconsistently apply thickness adjustments to each grade of steel (3). Thickness corrections should be included in material toughness specifications to ensure adequate fracture toughness. For the example presented herein, fracture toughness is adjusted for the plate thickness. The thickness correction is integrated into the above BS 7910 correlation; however, the correction can be independently applied if another correlation method is used.

Probability of Failure

The same phenomenon causing fracture toughness to be thickness dependent also allows for a statistical

treatment of cleavage fracture behavior. Probability of cleavage fracture occurrence in ferritic steel can be predicted through the use of a Weibull distribution, forming the basis of the master curve tolerance bounds (9). Applicability to historic bridge steel fracture data was validated in previous research (15). The statistical nature of fracture behavior allows for a reliability analysis of the fracture limit state.

For the current example, different failure probabilities were evaluated. To represent the lower bound of material performance, a five percent tolerance bound was selected as the control value. No explicit calculations for a five percent POF are necessary when using the above BS 7910 correlation. The selected correlation was developed for a five percent POF; however, other CVN-K correlation methods would require an explicit calculation of failure probability. Conversely, to represent a "best-fit" of fracture toughness data, a 50 percent POF was also included. The 50 percent POF was calculated using the master curve Weibull distribution.

Rate

In addition to temperature and material thickness, fracture toughness is also dependent on loading rate. Steel fracture toughness has an inverse relationship to loading rate, exhibiting a decrease in toughness as the applied loading rate is increased. Specimens loaded at a dynamic rate have significantly less fracture toughness than the same material loaded at a quasi-static rate. Historically, it has been accepted bridge loads are applied at a rate corresponding to a time of approximately one second to reach maximum load. The influence of loading rate is commonly represented by shifting fracture toughness data with respect to its test temperature, such as in the Barsom and Rolfe Two-Stage correlation.

A widely accepted rate adjustment for fracture toughness was proposed by Wallin, verified by others, and standardized in the master curve test method ASTM E1921 (14,16–18). The control case of the current example is based on static fracture toughness; however, the historic bridge loading rate corresponding to one second to maximum load was examined using the Wallin rate adjustment.

Fracture Mechanics

Calculation Approach

Evaluation of component or structural failure due to a fracture event is examined using fracture mechanics. A variety of analysis options exist, ranging from simple to extremely complex in application including linear-elastic fracture mechanics (LEFM), elastic-plastic fracture mechanics (EPFM), fitness-for-service (FFS) methodologies, and advanced 3-D finite element analysis (FEA).

LEFM Solutions

Evaluation of the fracture limit state for steel highway bridges has historically been based on linear-elastic fracture mechanics. LEFM analyses use known solutions for various geometries to determine an applied stress intensity factor, K, using the following generalized format:

$$K = \beta\sigma\sqrt{\pi a}$$

where β is a geometry factor, σ is the applied nominal stress, and a represents crack size. The calculated stress intensity is compared with the material fracture toughness in a one-dimensional analysis. LEFM is unable to capture material plasticity and can produce unconservative results as the applied stress approaches and surpasses approximately half of the material yield strength. However, simplicity in application makes the approach appealing.

Finite Element Analysis

At the other end of the fracture evaluation spectrum is the use of advanced 3-D finite element analyses (FEA). Modern software has the ability to generate applied fracture loads in terms of the linear-elastic stress intensity or the elastic-plastic J-integral. However, the application of FEA methodologies are difficult and requires knowledgeable professionals.

FFS and Failure Assessment Diagrams

The concept of FFS is an overall approach to evaluating structures or components with existing flaws. The analysis methodology used in the present example employs a fitness-for-service process known as the failure assessment diagram (FAD). FADs have the ability to examine the final limit states of strength and fracture simultaneously, including the elastic-plastic interaction. Used in a variety of industries, FFS procedures are codified in two main specifications: *BS 7910 Guide to Methods for Assessing the Acceptability of Flaws in Metallic Structures* and *API 579 Fitness-For-Service* (13,19).

A FAD examines failure due to brittle fracture on one axis and plastic collapse on the other through normalized ratios of applied load and material

resistance. Previous work examined the applicability of FFS techniques to steel bridges (20).

Failure Load

Evaluation of a component for the fracture limit state requires an applied stress. While fatigue crack initiation and propagation depend on applied stress range, the stress used for a fracture evaluation should correspond with the largest anticipated load the structure will experience once the crack reaches critical size. Therefore, the stress due to the design service load is the absolute minimum value able to be considered. For a steel bridge, the load level is approximately 55 percent of design yield strength. However, bridges routinely experience permit loads exceeding $0.55F_y$, with many states allowing permit loads approaching 75 percent of design yield strength (5). Therefore, an applied failure stress is $0.75F_y$ was used for the control case in the current example.

Fatigue Life

Fatigue life is defined as the time it takes a flaw to grow to a critical size, including both initiation and propagation time. A number of factors including flaw type, initial size, cycle count, and stress range can influence fatigue life. Typically, fatigue life is quantified as the number of cycles to failure. Cycle count is meaningless when trying to establish an inspection interval because the amount of time to accumulate the cycles will be different for every bridge. Therefore, converting to a timescale using the average daily truck traffic (ADTT) enables an inspection interval to be established with multiple opportunities to identify a flaw prior to failure.

Flaw Type

Flaw type has a large influence on fatigue life and fracture behavior. The stress intensity varies based on crack geometry, leading to different fatigue crack growth rates and critical flaw sizes. Flaw shape is defined by depth and width. A crack encompassing the complete depth of a component is known as a through-thickness crack. Through-thickness cracks can be located either at the edge or anywhere along the width of a component. When located within the width of a component, the crack is typically referred to as a center crack. However, through fatigue, a center crack can grow to become an edge crack. Based on the location, the fatigue and fracture calculations are unique.

A partial depth crack is commonly referred to as penny-shaped. Penny-shaped cracks can be surface breaking or internal. Surface breaking penny-shaped cracks are visible from a single side of a component; whereas, internal cracks cannot be viewed without some form of non-destructive or destructive means. Again, based on the flaw location within a plate, the fracture mechanics differ.

Considering fatigue and fracture behavior, each crack geometry demonstrates unique performance. Looking at crack depth, through-thickness cracks have the largest demand, followed by surface breaking defects, and finally internal defects. Similarly, edge cracks have a larger demand than center cracks. Therefore, the worst-case crack geometry based solely on a fracture analysis is a through-thickness edge crack because it will generate the largest stress intensity. As such, the control specimen used in the current example is a through-thickness edge crack.

Initial Flaw Size

Critical crack size can be calculated through fracture mechanics with knowledge of the loading and material properties; however, setting an initial flaw size requires an assumption. Establishing an initial flaw has a large impact on the fatigue crack growth, and in turn, the resulting rational inspection interval. Fatigue crack growth rate increases with increasing crack length; as such, a large percentage of fatigue life is associated with a small percentage of crack growth. Further, a threshold exists for a given stress range at which an initial flaw will not propagate in fatigue. Therefore, the most difficult question is what initial flaw size is realistic. Any assumed initial flaw expected to result in fatigue crack growth would be large compared to what would be expected from a fabrication shop. However, a fracture mechanics-based assessment requires an initial flaw; therefore, the size must be set considering potential defects caused during erection or an extreme event, such as an impact. The example examines through-thickness flaw sizes ranging from 1/16 in. to 1/4 in. with the control initial flaw size set at 1/8 in.

ADTT

The fatigue life analysis will output life in terms of cycles. Unfortunately, cycles cannot be directly used to establish a rational inspection interval. Therefore, a conversion must be performed to represent the fatigue life in terms of time. The average daily truck

traffic is the source of the fatigue damaging cycles. As such, ADTT can be used to convert the fatigue life in cycles to a time-based interval. From the total fatigue level, an interval can be set to allow multiple opportunities to detect any potential defects.

An ADTT of 1000 was used throughout the life of the bridge in the current example. Previous research revealed an ADTT of 1000 represented 75% of all the bridges in Indiana (21). However, any ADTT value can be substituted using the simple conversion. For example, a small rural bridge may justify a smaller value, while a major Interstate bridge in a suburban area would need a much larger value.

Effective Stress Range

Once the critical flaw size has been determined and an initial flaw size has been established, the number of cycles required to grow to failure will depend on the effective stress range. Most modern steel bridges are designed to have fatigue performance better than a Category C detail. Category C assumes a stress range of less than 10 ksi will result in infinite life for a given detail. Realistically, the in-service live load stress range will be much lower. Based on field monitoring performed on several in-service structures 3 ksi was deemed to be realistic and reasonable (22–24). Therefore, the control case utilizes a stress range of 3 ksi, while higher and lower stress ranges are examined as part of the analysis.

Example

Input

A parametric analysis was performed to evaluate the impact different input parameters have on the calculated fatigue life of a bridge structure. The study did not include all parameters previously discussed; rather, the analysis was limited to initial flaw size, fracture stress, probability of failure due to fracture, fatigue stress range, flaw type, and loading rate adjustment. The resulting test matrix can be found in Table 1. The first row of the table is a control specimen used as the basis of comparison. The parameter(s) evaluated for each case was highlighted in grey in the matrix. It should be noted, all fracture toughness values are based on the BS 7910 CVN-K correlation and impact toughness of 125 ft-lbf tested at the MST.

Specimen	Initial Flaw Size (in.)	Grade 50 Fracture Stress (ksi)	Probability of Failure	Stress Range (ksi)	Shape	Fracture Toughness (ksi√in)
Control	1/8	37.5	5	3.0	Through-thickness Edge	122.4
Small Flaw	1/16	37.5	5	3.0	Through-thickness Edge	122.4
Big Flaw	1/4	37.5	5	3.0	Through-thickness Edge	122.4
Low Stress	1/8	27.5	5	3.0	Through-thickness Edge	122.4
High POF	1/8	37.5	50	3.0	Through-thickness Edge	217.3
Low SR	1/8	37.5	5	1.0	Through-thickness Edge	122.4
High SR	1/8	37.5	5	5.0	Through-thickness Edge	122.4
Flaw Type	1/8	37.5	5	3.0	Through-thickness Center	122.4
Flaw Type and Size	1/4	37.5	5	3.0	Through-thickness Center	122.4
Rate	1/8	37.5	5	3.0	Through-thickness Edge	79.2

Table 1: Parametric analysis test matrix

Signal Fitness-For-Service (Signal FFS) software was used for all fracture and crack growth assessments, automating the engineering critical assessment procedures found in BS 7910. Several parameters were held constant for all calculations. The width and thickness used in the computations were 18 in. and 2 in., respectively. For non-redundant steel bridges, the selected plate size represents a lower bound flange width and average flange thickness. All geometries were modeled in Signal FFS as flat plates with cracks perpendicular to stress. Welds were not considered for the analysis and the flaw location was in parent metal remote from any welds. The selected material was steel in air with a modulus of elasticity of 29,000 ksi. Tensile properties for all analyses were defined as 50 ksi yield strength and 65 ksi ultimate strength.

The ratio of the minimum to maximum stress intensity is known as the R-ratio. To consider residual stress, the R-ratio was assumed to be greater than 0.5, which is appropriate for in-plane fatigue loading in bridges. The BS 7910 fatigue coefficients at a temperature of 70 °F were used with a piece-wise power law crack growth model (13). The specified threshold stress intensity value of 1.813 ksi√in was utilized. None of the other the coefficients related to fatigue crack growth were altered from BS 7910.

Results and Discussion

Results from the integrated FCP parametric study are presented in Table 2, including the critical crack length, number of cycles to failure, and fatigue life in years for an ADTT of 1000. For cases where no crack growth was calculated, "Infinite Life" was indicated. Three cases resulted in infinite life including the small flaw size of 1/16 in., low stress range of 1.0 ksi, and the center-crack geometry.

Specimen	Critical Crack Length (in.)	Number of Cycles	Life for ADTT of 1000 (years)
Control	1.3	30,638,280	83.9
Small Flaw	1.3	Infinite	Infinite Life
Big Flaw	1.3	10,906,402	29.9
Low Stress	2.6	32,506,290	89.1
High POF	2.3	32,236,956	88.3
Low SR	1.3	Infinite	Infinite Life
High SR	1.3	3,595,353	9.9
Center	3.1	Infinite	Infinite Life
Flaw Type and Size	3.1	54,583,128	149.5
Rate	0.7	27,949,424	76.6

Table 2: Parametric analysis results

Initial flaw size and stress range had the greatest influence on the fatigue life. Evaluating the impact of the initial flaw size, the 1/16 in. initial crack resulted in no growth. However, as expected, increasing the initial crack size dramatically reduces the calculated life. Figure 1 plots the fatigue life in years for a stress range of 3 ksi, 1/8 in. initial crack, and ADTT of 1000 versus the crack length. Results for some of the specimens can be extracted from the curve. The plot demonstrates how the majority of the fatigue life occurs for short crack lengths. For example, growing a crack from 1/8 in. to 1/4 in. takes approximately 50 years. Conversely, growing the crack another 1/8 in. takes less than 20 additional years. Due to crack growth being exponential in nature, the crack growth rate increases for increasing crack length. As such, changing the initial flaw size even 1/16 in. can have a dramatic impact on the fatigue life.

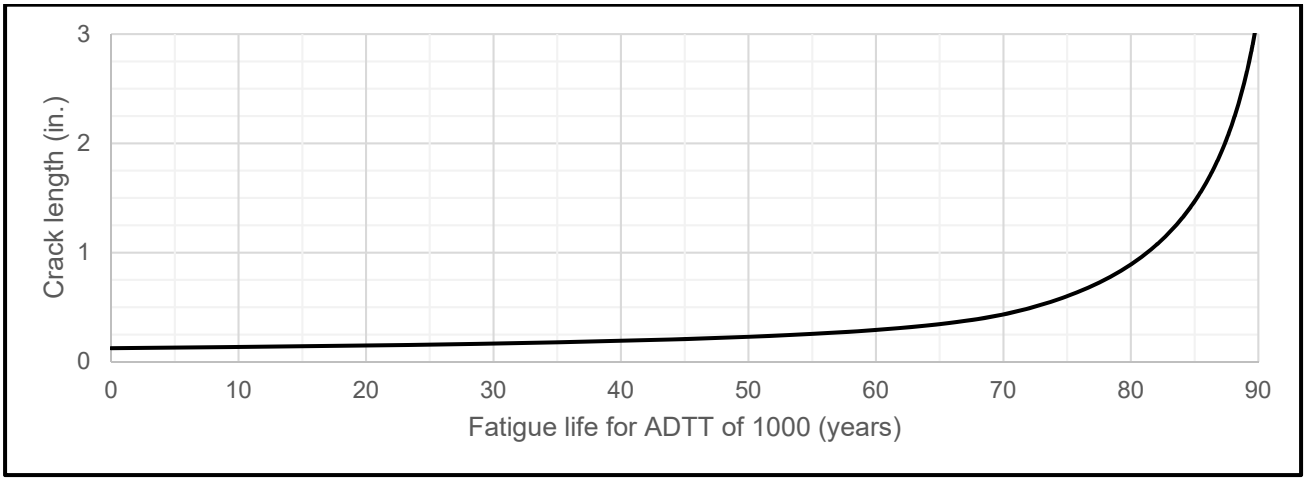

Figure 1: Fatigue life in years versus crack length

The second parameter having a large impact on the fatigue life is stress range. The low stress range of 1.0 ksi resulted in infinite life compared to 83.9 years calculated for the control stress range of 3.0 ksi. However, increasing the stress range to 5.0 ksi produced a fatigue life of only 9.9 years.

To evaluate the impact of stress range further, analyses were conducted for stress range values from 1.0 to 5.0 ksi in 0.5 ksi increments. The results of the stress range study are presented in Table 3. Interestingly, infinite life is achieved for all stress ranges below the control value of 3.0 ksi. However, for all stress ranges above 3.0 ksi the fatigue life decreases at an exponential rate. The behavior is explained by Paris' law, which defines incremental crack growth with an exponential function of applied stress intensity, which is linearly related to applied stress. Compounding the exponential growth is the fact stress intensity is not constant during fatigue propagation, but increases with increasing crack size. Therefore, incremental increases in stress range result in significant reductions to fatigue life.

Stress Range (ksi)	Number of Cycles	Life for 1000 ADTT
1.0	Infinite	Infinite Life
1.5	Infinite	Infinite Life
2.0	Infinite	Infinite Life
2.5	Infinite	Infinite Life
3.0	30,638,280	83.9
3.5	14,972,382	41.0
4.0	8,395,112	23.0
4.5	5,257,159	14.4
5.0	3,595,353	9.9

Table 3: Stress range evaluation

The parameters of fracture stress, POF, and loading rate had little impact on the overall fatigue life. All three parameters affect the fracture toughness, thereby influencing the critical crack length. Referring to Figure 1 and the above discussion explains why little change in fatigue life is attained when fracture stress, POF, and loading rate are changed. The exponential shape of the fatigue life versus crack length curve dictates the result. Once the crack reaches 3/8 in., the length grows rapidly with negligible change in the fatigue life. However, the results do not imply fracture toughness is unimportant; rather, a minimum level of fracture toughness is required to reach the exponential portion of the crack growth curve.

Flaw type was the final parameter evaluated during the study. As expected, changing from an edge crack to a center crack made a notable difference in the fatigue life results. For a through-thickness center crack having a width of 1/8 in., infinite life was achieved. The geometry of the center crack results in a lower stress intensity compared with the edge crack, which does not exceed the threshold for crack growth. Additional supporting analysis was performed which revealed increasing the center crack to 1/4 in. resulted in a fatigue life of 149.5 years and final crack length of 3.1 in. The results of the additional analysis demonstrate the impact of flaw type on fatigue life.

Future Implementation

Applying a rational inspection interval is beneficial to bridge owners. Rather than arbitrarily performing an in-depth fracture critical inspection every two years, a rational inspection interval can be established using a quantitative basis. For example, the control specimen has a fatigue crack life longer than the 75-year bridge service life, indicating no special hands-on fracture critical inspection is required during the bridge service life. As such, routine bridge inspections only need to be performed to identify other forms of degradation such as corrosion, impact damage, or scour.

While never inspecting a bridge for fatigue and fracture is possible, it may not always be feasible, or an owner may not be comfortable with such a drastic change in policy. Therefore, the integrated FCP methodology can still be applied to more rationally set an interval for in-depth inspection. Using the control specimen as an example, an owner who wants at least 10 opportunities to identify a crack prior to it reaching the critical length of 1.3 in. simply divides the total fatigue life of 83.9 years by 10 inspection cycles to set an inspection interval of 8 years. Regardless of the interval, it is clear inspecting for small fatigue cracks at a 24-month interval in a modern steel bridge built using an integrated FCP is not an efficient use of resources.

A quantitative calculation of fatigue life is only one of two major aspects of the rational inspection approach. The second key is establishing the critical flaw size. By knowing the critical flaw size, the inspection rigor and method can be tailored

accordingly. For example, when comparing Figure 1 to existing POD data for visual inspection it is unlikely the visual method would reliably identify the critical defect for the first 80 years of life (25). Therefore, a method, such as magnetic particle inspection or ultrasonic inspection, with an appropriate POD should be employed. Using an integrated FCP, inspection technique can be rationally tied to the critical flaw size.

Conclusion

Advances made since the inception of the 1978 FCP now allow fracture to be treated like any other reliability-based limit state. For such a paradigm shift, fracture must be treated in an integrated fashion. First, it must be recognized and accepted defects exist, bridge loading is variable, materials are variable, and both shop and in-service inspection methods have limitations. However, the components of an integrated FCP can mitigate such realities. The required components of an integrated FCP include design considerations, material properties, fabrication guidelines, and in-service inspection. A framework was presented for establishing rational inspection intervals. The various parameters and assumptions involved in the calculation were explored. Finally, a parametric analysis was presented demonstrating the influence of each parameter on the interval calculation. Leveraging modern advances can revolutionize how fracture is treated in the steel bridge industry. Ultimately, an integrated FCP with rational inspection intervals will increase bridge safety and allow for a better allocation of owner resources.

References

1. AASHTO. Guide Specificaitons for Fracture Critical Steel Bridge Members. Washington, DC: American Association of State Highway and Transportation Officials; 1978.
2. AASHTO. AASHTO LRFD Bridge Design Specification. 8th ed. Washington, DC: American Association of State Highway and Transportation Officials; 2017.
3. ASTM. ASTM A709-17: Standard Specification for Structural Steel for Bridges. ASTM Stand; 2017.
4. AASHTO A. AASHTO/AWS D1.5 Bridge Welding Code. 7th ed. American Welding Society; 2015.
5. AASHTO. The Manual For Bridge Evaluation. 2nd ed. Washington, DC: American Association of State Highway and Transportation Officials; 2011.
6. Wilson A. Improvements to High Performance Steels by. Vol. 110. 2005.
7. Wright WJ. Fracture Initiation Resistance of I-girders Fabricated from High-Performance Steels. Lehigh University; 2003.
8. Connor RJ, Collins WN, Sherman RJ. TPF-5(238): Design and Fabrication Standards to Eliminate Fracture Critical Concerns in Two Girder Bridge Systems - Fracture Characterization of High Performance Steel. West Lafayette, IN; 2015.
9. McCabe DE, Merkle JG, Wallin K. Technical basis for the master curve concept of fracture toughness evaluations in the transition range. Fatigue Fract Mech 30th Vol ASTM STP 1360. 2000;30:21–33.
10. Connor RJ, Sherman RJ, Collins WN. TPF-5(238): Design and Fabrication Standards to Eliminate Fracture Critical Concerns in Two Girder Bridge Systems - Experimental Testing. West Lafayette, IN; 2016.
11. FHWA. 23 CFR §650.311. 2013 p. Federal Register.
12. Collins WN, Sherman RJ, Leon RT, Connor R. State-of-the-Art Fracture Characterization. II: Correlations between Charpy V-Notch and the Master Curve Reference Temperature. J Bridg Eng. 2016;21(12).
13. BSI. BS7910:2013 - Guide to Methods for Assessing the Acceptability of Flaws in Metallic Structures. 3rd ed. British Standards Institution; 2013.
14. Wallin K. Fracture Toughness of Engineering Materials: Estimation and Application. EMAS Publications; 2011.

15. Collins WN, Sherman RJ, Connor RJ, Leon RT. State-of-the-Art Fracture Characterization. I: Master Curve Analysis of Legacy Bridge Steels. ASCE J Bridg Eng. 2016;21(12).

16. Gao X, Joyce JA, Roe C. An investigation of the loading rate dependence of the Weibull stress parameters. Eng Fract Mech. 2008;75(6):1451–67.

17. Gao X, Dodds RH. Loading rate effects on parameters of the Weibull stress model for ferritic steels. Eng Fract Mech. 2005;72(15):2416–25.

18. ASTM. ASTM E1921-17a: Standard Test Method for Determination of Reference Temperature, To, for Ferritic Steels in the Transition Range. ASTM B Stand. 2017;1–27.

19. API. API 579-1 Fitness-For-Service. American Petroleum Insitute; 2016.

20. Collins WN, Sherman RJ, Connor RJ. Advancing the State of Practice in Steel Bridge Evaluation: Application of the Master Curve and Fitness-for-Service for Existing Structures. World Steel Bridg Symp; 2016.

21. INDOT. Indiana Department of Transporation Bridge Inventory Database. Indianapolis, IN; 2014.

22. Sherman RJ, Mueller JM, Connor RJ, Bowman MD. Evaluation of Effects of Super-Heavy Loading on the US-41 Bridge over the White River. West Lafayette, IN; 2011.

23. O'Connell H, Dexter R, Bergson P. Fatigue evaluation of the deck truss of bridge 9340. Civ Eng; 2001.

24. Fasl J, Helwig T, Wood SL, Frank K. Use of Strain Data to Estimate Remaining Fatigue Life of a Fracture-Critical Bridge. Transp Res Rec J Transp Res Board. 2012;2313(1):63–71.

25. Whitehead J. Probability of Detection Study for Visual Inspection of Steel. West Lafayette, IN: Purdue University; 2015.